Impact of sand on the water retention properties of a bentonite/sand mixture by NMR characterization

Pablo Eizaguirre, Anh Minh Tang, Benjamin Maillet, Rahima Sidi-Boulenouar, Baptiste Chabot, Michel Bornert, Jean-Michel Pereira, Patrick Dangla, Patrick Aimedieu, Jean Talandier, et al.

Impact of sand on the water retention properties of a bentonite/sand mixture by NMR characterization

Pablo Eizaguirre[1,2*], *Anh Minh* Tang[1], *Benjamin* Maillet[1], *Rahima* Sidi-Boulenouar[1], *Baptiste* Chabot[1], *Michel* Bornert[1], *Jean-Michel* Pereira[1], *Patrick* Dangla[1], *Patrick* Aimedieu[1], *Jean* Talandier[2] and *Minh Ngoc* Vu[2]

[1]Navier Laboratory, Ecole des Ponts, Univ Gustave Eiffel, CNRS, Marne-la-Vallée, France
[2]French National Radioactive Waste Management Agency (Andra), Châtenay-Malabry, France

Abstract. Blocks of compacted bentonite/sand mixture, with a 40/60 proportion in dry mass, are being studied as an elementary component in the construction of seals in the French concept for high-level radioactive waste disposal. In the disposal, the seal will be subjected to water infiltration from the host rock. Water retention behaviour in the mixture is governed by bentonite. Nevertheless, the impact of the sand fraction, especially at high concentrations, is still unclear. The water retention curve is found experimentally for the wetting path by using vapour equilibrium technique. Moreover, NMR relaxometry tests executed at full saturation state are presented. As a result of the comparison with experimental data reported in the past, for different mixtures -ranging from pure bentonite to 20/80 bentonite/sand mixtures-, it is concluded that all porosity in the mixture can be correctly attributed to bentonite. This conclusion simplifies mixtures to equivalent pure bentonite specimens with a dry density equal to the bentonite dry density ($\rho_{d,b}$) of the mixture. Moreover, an original method to compare NMR relaxation times for different bentonite/sand -or pure bentonite- mixtures is proposed. It provides the longitudinal relaxation time (T_1) in saturated mixtures as a function of $\rho_{d,b}$ and the montmorillonite concentration in bentonite.

1 Introduction

Precompacted bentonite/sand mixture, with proportions of 40/60 on dry mass, is a potential candidate material in the construction of multibarrier systems in the French concept for high-level radioactive waste disposal conducted by Andra. The barrier will be subjected to a slow hydration process limited by water -both liquid and vapour- infiltration from the host rock. Water retention properties play a crucial role on the hydromechanical behaviour during the hydration of clayey soils, as it is the case for bentonite mixtures.

Bentonite fraction in the mixture contributes to have a low permeability material with high swelling capacity [1]. These are feature properties of engineered barriers. Sand fraction contributes improving mechanical stability, reducing the amount of bentonite required [2] and, possibly, improving its performance to gas migration phenomena.

Water retention curve (WRC) summarizes the hydric response of a porous material, typically clayey soils. It defines the retention properties of porous medias, relating suction values with water content. Experimental data from bentonite/sand mixtures have been reported in the past, including analyses of parameters as the bentonite dry density, ($\rho_{d,b}$) [3].

Bentonite dry density was defined by [4] as the mass of bentonite divided by the sum of its volume and the volume of pores in the mixture. Other authors have used it, as well, to characterize hydromechanical properties of bentonite/sand mixtures. The attribution of the entire porosity to the bentonite fraction implies that bentonite swells, filling it. This assumption is reasonable but needs to be verified for mixtures with high proportions of sand.

Physicochemical interactions between water and clay particles strongly depend on pore distribution characteristics. Thus, a campaign of Nuclear Magnetic Resonance (NMR) relaxometry experiments was conducted with the aim of analysing the dynamics of porewater populations at saturation state. NMR relaxometry consists of a non-destructive measurement of the time it takes to magnetization of molecules to return to equilibrium after having been subjected to a radio frequency wave, at a frequency equal to the resonance frequency, in a magnetic field. When applied to water in porous media, it correlates porewater properties with relaxation times by translating measurements from hydrogen protons to water population analysis.

Other authors have studied the NMR relaxometry of smectites in the past. However, there are still important gaps to properly interpretate the results [5]. Moreover, bentonite/sand mixtures are rarely studied with the NMR technique.

* Corresponding author: pablo.eizaguire-garcia@enpc.fr

The influence of sand on the water retention properties, especially on mixtures with high proportions of sand, is not clear yet.

This publication analyses the sand influence on the water retention properties on bentonite/sand mixtures, by proposing two hypotheses and testing them experimentally by comparing water retention curves and NMR relaxometry results of different bentonite/sand mixtures. Analysis includes materials from pure bentonite to mixtures with 20% of bentonite -on dry mass-. For this purpose, original comparison methods are proposed as well.

2 Methodology

In the following, the procedures followed during the experimental campaign are described chronologically, starting with the material preparation, then the relaxometry scanning and finally, the water content measurement. The methodology is designed to run NMR tests on specimens at different suction values. However, only NMR tests at saturation state are presented.

2.1 Material

The material studied is a compacted mixture of WH2 gelclay bentonite from Wyoming and TH1000 sand. The proportions in dry mass are 40/60 (bentonite/sand). The mixture was provided by Andra in form of blocks with dimensions of 300 x 200 x 100 (mm^3). The blocks had been precompacted at 80 MPa in an industrial process. The dry density of the blocks is ρ_d = 2.03 g/cm^3. The bentonite has a particle density γ_b = 2.77 g/cm^3. It has a sodium Na^+ governed cation exchange capacity and is assumed to have a smectite content of 80 %. The sand is a quartz sand with a particle density γ_{sand} = 2.65 g/cm^3. The bentonite and sand fractions have similar granulometric curves. The mean grain diameters are respectively, for the bentonite and the sand, D_{50}^{b}= 0.90 mm and D_{50}^{sand}= 0.55 mm.

Small samples were prepared to fit the limit diameter of the NMR instrumentation and its optimal height -taking into account that the apparatus measurements are limited to 10 mm height-. This way, 12 mm diameter and 10 mm height samples were prepared. For this purpose, a diamond saw was used to cut slices of 10 mm thickness. Then, manual saw and sand paper were used to arrive to the desired final dimensions measured with a precision calliper.

The initial water content of the mixture, 7.17 %, was measured by oven drying at 105 °C. The measured initial suction was 66 MPa using a dew point chilled-mirror potentiometer WP4C (Decagon Device Inc., 2).

Due to the importance of dry density in the water retention behaviour, the samples were placed inside a plastic cell, produced by a 3D printer, that prevented the uncontrolled swelling of the samples, when submitted to high relative humidity states.

For the saturation state sample, the plastic cell was not able to resist the swelling pressure of the sample. So, a bentonite/sand mixture, with the same properties, was compacted inside an oedometer cell. Inside, hydration until saturation state can be reached at constant volume conditions. The saturation state is considered to be reached once the permeability of the sample is stable. This phenomenon was observed by the water infiltration applied to hydrate the sample, with a pressure-volume controller system (GDS). This process took 3-5 days. Afterwards, the suction was measured in the dew point chilled-mirror potentiometer. A value of 0.1 MPa of suction was determined to fit best after some reproductivity tests were done.

2.2 Suction imposed samples

To reproduce the hydration states of the material along the wetting path, the vapour equilibrium technique is used [6]. It is based on placing the sample inside a closed recipient filled partially with a saturated saline solution. The air inside the recipient will set to a known relative humidity.

A list of saline solutions presented in Table 1 was used, providing enough values of relative humidity to characterise the wetting path of the material. Meanwhile, corresponding to each relative humidity state, it is possible to obtain its suction value imposed to the porous media by using the Kelvin law.

Table 1. Saline solutions used to control suction by vapour equilibrium technique

Salt	Relative Humidity (%)	Suction (MPa)
K_2CO_3	44	113
$Mg(NO_3)_2$	55	82
$NaNO_2$	66	57
NaCl	76	38
$NaNO_3$	75	30
$(NH_4)_2SO_4$	83.5	25
KNO_3	93.7	9
K_2SO_4	97.0	4

So, the samples were placed inside desiccators containing each of the saline solutions in a temperature-controlled room set to 20 °C. Each sample, above the saline solution, enters in a water exchange which takes place by vapour phase. Once a week the plastic cell containing the sample was weighed until mass equilibrium was reached -same mass in consecutive weighs with a precision of 0.01 g-. The plastic cell absorbed water so it represented an extra volume of water exchange that made the experiment take longer to get to equilibrium. However, the final water content of the sample stored inside is not affected. In fact, the cells included small holes to facilitate the water exchange. The vapour equilibrium process took 85 days.

2.3 NMR scanning

2.3.1 Fundamentals and instrumentation

The instrumentation used in the experiments is a Bruker low-field NMR Minispec mq20, 0.5T working at a frequency of 20 MHz. Its measured volume is limited to 1 cm^3 approximately. Longitudinal relaxation time (T_1) is obtained from measures of a modified Inversion Recovery (*IR*) sequence. Each sequence has 100 measures distributed logarithmically from 0.16 ms to 1000 ms. The number of scans during the sequence is 64 to optimize the signal-to-noise ratio. Transverse relaxation time (T_2) is obtained from measures of a Carr-Purcell-Meiboom-Gill (*CPMG*) sequence composed of a first "$\pi/2$" pulse and 1000 "π" pulses distributed linearly up to 200 ms. The repetition time is 10 s to get a complete relaxation of all protons. The number of scans in this case is 256, to increase the signal-to-noise ratio. Furthermore, a bidimensional sequence which applies both IR and CPMG was used to plot a graph corresponding to the signal in function of both T_1 and T_2. The study of both T_1 and T_2 provides a clear observation of porewater populations, whereas the measures of T_1 or T_2 separately, are faster to run and easier to quantify.

The relaxation time distribution is only available after treating the data through inverse Laplace transform [7, 8]. Signal intensity value shape depends on the regularization technique, particularly in the parsimony factor. However, it does not affect the position of peaks or the integral below the peak [9].

2.3.2 Relaxometry tests

Once at saturation state, the sample is weighed and covered with Teflon to prevent any water exchange during the relaxometry test. Moreover, after the test -whose duration was three hours-, the sample was weighed again and it was verified that it did not experience any appreciable water exchange -bigger than 0.01 g-. During the tests, samples were at 20 °C of temperature, thanks to the apparatus temperature control system.

Potentially identified populations of water are characterised by a peak value. This is determined by statistic treatment to be the most representative relaxation time of each water population. It does not correspond exactly with the maximum value of the peak shown in the graphs as the distributions are not symmetrical.

2.4 Water retention

This phase starts after imposing suction to the samples by vapour equilibrium technique. In the case of the saturated sample, it is done after the NMR test.

The water content is calculated by Equation 1 where m_d is the dry mass and m_w is the mass of water in the sample estimated as the total mass subtracted by the dry mass. The samples are weighed with digital balance. The dry mass is estimated after oven-drying 24 hours at 105 °C.

$$w = {}^{m_w}/_{m_d} \tag{1}$$

2.4.1 Hypothesis of sand effect in the mixture

The first hypothesis is that sand fraction is not able to retain water in the compacted mixture. Thus, the bentonite fraction is assumed to absorb all the water in the sample.

This model introduces the parameter w_b denominated as bentonite water content. It is defined as the water content of the mixture, *w*, divided by the bentonite dry mass proportion in the mixture, *B*, as shown in Equation 2. In other words, it is the relation of water mass with bentonite mass.

$$w_b = {}^{w}/_{B} \tag{2}$$

The second hypothesis is that all porosity in the sample can be attributed to the bentonite. Whereas the sand fraction is considered inert, the bentonite fraction swells during hydration, filling the gaps of porosity.

From this hypothesis, results the parameter $\rho_{d,b}$, named bentonite dry density, or effective bentonite dry density. It is defined as the dry mass of bentonite divided by the sum of the volume of bentonite and the volume of pores in the entire mixture. From this definition, Equation 3 is deduced:

$$\rho_{d,b} = \frac{B\ \rho_d\ \gamma_{sand}}{\gamma_{sand} - \rho_d(1-B)} \tag{3}$$

For pure bentonite mixture, use $B = 1$. γ_{sand} is the particle density of sand and ρ_d corresponds to the dry density of the mixture. It is an enhanced formulation - does not depend on the water content or the water density- of similar expressions found in [4, 10-11]. The proposed expression fits better with the compaction process application where, usually, the control variable is the dry density.

2.4.2 Testing the hypotheses

The resulting WRC is compared with other authors' observations from mixtures with different proportions of bentonite, and even pure bentonite, using the w_b parameter instead of *w*.

Similar w_b values resulting from the different mixtures are expected to verify the first hypothesis.

To test the second hypothesis, the bentonite dry density ($\rho_{d,b}$) behaviour is compared to the classic dry density influence on the WRCs of high-compacted bentonite mixtures at constant volume conditions. To quantify this influence, the maximum value of water content possible to reach at constant volume conditions, so at saturation state (w_b^{sat}), is estimated via $\rho_{d,b}$. The resulting parameter, is named as saturated bentonite water content. It is calculated by the Equation 4, which assumes the mass of water to be equal to the porosity volume multiplied by the density of water, ρ_w. Density of water is considered constant and equal to 1 g/cm^3 in this publication. γ_b is the bentonite particle density.

$$w_b^{sat} = \left(\frac{\gamma_b}{\rho_{d,b}} - 1\right)\frac{\rho_w}{\gamma_b} \quad (4)$$

Whether the bentonite water content resulting from the WRCs, at saturation state, is equal to the calculated w_b^{sat}, the second hypothesis is verified.

3 Results

Firstly, water retention behaviour is presented in form of water retention curve. Following, NMR relaxation time distributions at saturation state are presented. In both cases, the interpretation is supported by comparison with bibliographic data.

3.1 Water retention curve (WRC)

3.1.1 Raw results

The Figure 1 shows the results obtained from the water retention determination. It compares the suction values on a logarithmic scale, with the water content obtained. This represents the evolution of the capacity of the soil to absorb water when submitted to increasingly humid environments -with relative humidity ranging from 44% to 100%, at complete saturation-.

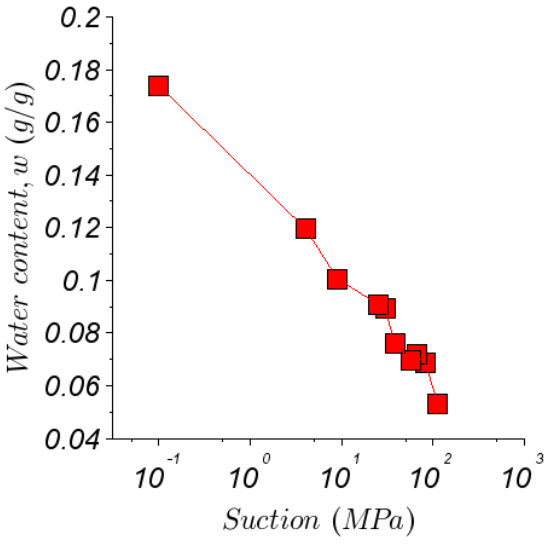

Fig. 1. Measured WRC along the wetting path

It is observed a linear behaviour all along the wetting path. This behaviour is well reported in free swelling experiments. On the contrary, constant volume tests highlight an asymptotic shape at low suctions towards a water content dependent of the dry density [12]. The suction value corresponding to the transition point between those two regimes depends on the bentonite dry density of the sample.

The discrepancy between the results obtained -representing free swelling (linear behaviour)- and the results expected -constant volume (linear and asymptotic behaviour)- was observed to be due to swelling experienced in the hydration of the saturated sample. Therefore, water content at suction 0.1 MPa is overestimated if compared to a constant volume test.

3.1.2 Comparative results

Following, Figure 2 presents the results of this study, at the same time as experimental data from [3, 13-14] obtained from tests at constant volume for different mixtures, whose characteristics are summarized in Table 2. The resulting w_b is similar at suctions bigger than 9 MPa for all mixtures. This reflects that sand does not absorb water in this range of suctions. For suctions lower than 9 MPa, the WRCs diverge to different w_b values corresponding to the saturation state. These values are very close to those found theoretically by the term w_b^{sat}, and presented in Table 2. The only experimental data that does not correspond to the theoretical value is the one from the present study. This is due to the consideration of constant volume conditions when calculating w_b^{sat}, which underestimates the experimental measurements. Thus, a proof that swelling occurred during the sample wetting.

WRCs show the influence of the bentonite dry density on the suction value corresponding to the transition point where a WRC starts to change from its linear behaviour to an asymptotic one -the higher is the bentonite dry density, the higher the suction would be-.

Table 2. Theoretical values of bentonite dry density and saturation bentonite water content calculated for the different mixtures

Publication	ρ_d (g/cm^3)	B (g/g)	$\rho_{d,b}$ (g/cm^3)	w_b^{sat} (g/g)
Manca (2015)	1.80	0.2	0.79	0.90
This study	2.03	0.4	1.50	0.31
Wang et al. (2013)	1.67	0.7	1.45	0.33
Tang & Cui (2010)	1.65	1	1.65	0.25

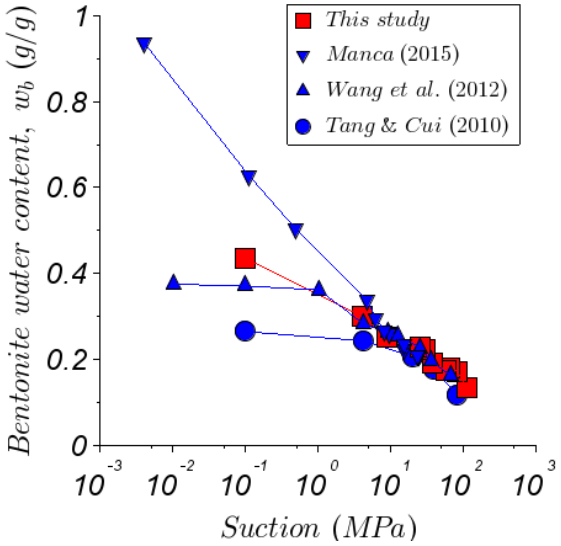

Fig. 2. Measured WRC along the wetting path compared with bibliographic -constant volume conditions- experimental data from [3, 13-14].

3.2 NMR relaxometry

3.2.1 Results at saturation state

The results of the relaxometry test at saturation state are presented in Figure 3. They show a single population of porewater characterised by T_1 = 2.32 ms and T_2 = 2.31 ms. The T_1-T_2 map highlights the uniform signal of the single population captured. This observation is in agreement with pure bentonite results from [15-18].

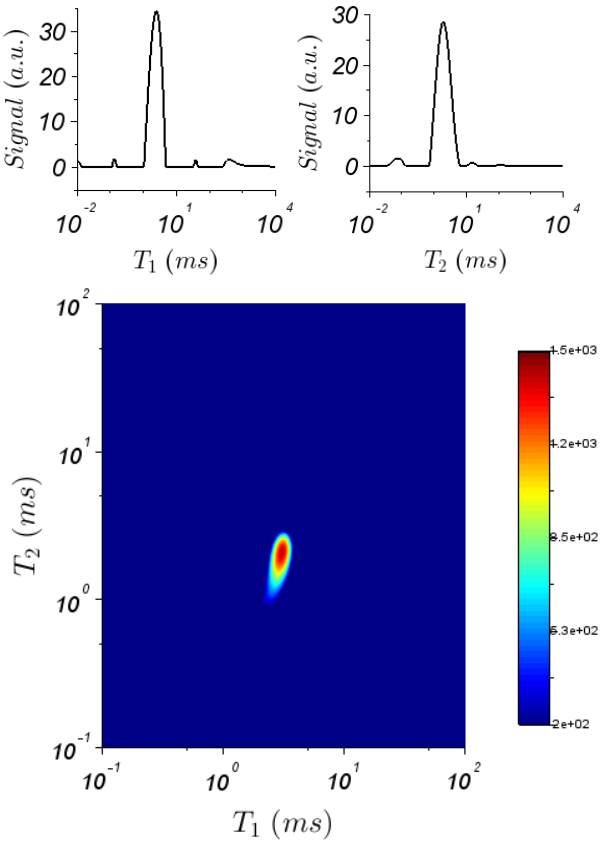

Fig. 3. NMR relaxometry results at saturation state

Porewater populations found using NMR have successfully been related to pore size distributions in other materials such as hardwood [8], where water fills different pore populations, each one with its own molecular dynamics. In the case of bentonite, it is reported the existence of different pore population with, indeed, different molecular dynamics -interlayer pores and interaggregate pores- [19]. However, single molecular dynamics is observed, despite the fact that macropore water dynamics are understood as more dynamic than water stored between the layers of clay. The interlayer water is well-known to be strongly bounded to montmorillonite layers. So, a possible reason to explain why NMR relaxometry does not identify the difference between the porewater populations is that there is a fast diffusion exchange between them [15]. This would mean that the relaxation time observed is, in fact, the average relaxation time of the different porewater populations.

3.2.2 Comparison with pure bentonite mixtures

Relaxation times depend on the dry density of the mixture and temperature during the test, as proved experimentally by [20] and [17, 21] respectively. Considering that all tests were done at 30 °C, a comparative analysis of relaxation times for pure bentonite and bentonite/sand specimens is proposed. Only longitudinal relaxation time T_1 at saturation state is regarded as T_2 results, for bentonite/sand mixtures, are not reported in the literature.

So, Figure 4 and Figure 5 show the dependency of bentonite dry density ($\rho_{d,b}$) on the longitudinal relaxation times measured. Increase on relaxation time is related to more dynamic porewater and larger pores. Results shown for the WB2 and sand mixture are compared with experimental data reported in [20], which corresponds to NMR experiments made in three different mixtures: Kunipia-F, Kunigel-V1 and Kunigel-V1 with sand (B = 70%) -all of them at saturation state-. The montmorillonite concentration is, 98% and 60%, respectively, for the Kunipia-F and the Kunigel-V1 bentonites.

A remarkable similarity between values found from pure bentonite and bentonite-sand mixtures is observed. In fact, Figure 4 highlights that the Kunigel-V1 observations are similar for the mixture with sand and without it. Nevertheless, observations from other bentonites are not similar, remarking that Kunipia-F relaxes faster. So, the nature of bentonite is appreciably more impactful than the presence of sand.

Relative to the nature of the bentonites analysed, relaxation time values are shown in Figure 5, in this case, multiplied by the montmorillonite concentration in the bentonite (C_{mmt}). All mixtures present the same behaviour. By decreasing the density, relaxation time increases exponentially for every mixture, defining a curve where results for all mixtures collapse on a single curve. Thus, the sand fraction does not influence the NMR results. Moreover, montmorillonite content seems to play a major role in the relaxation time results.

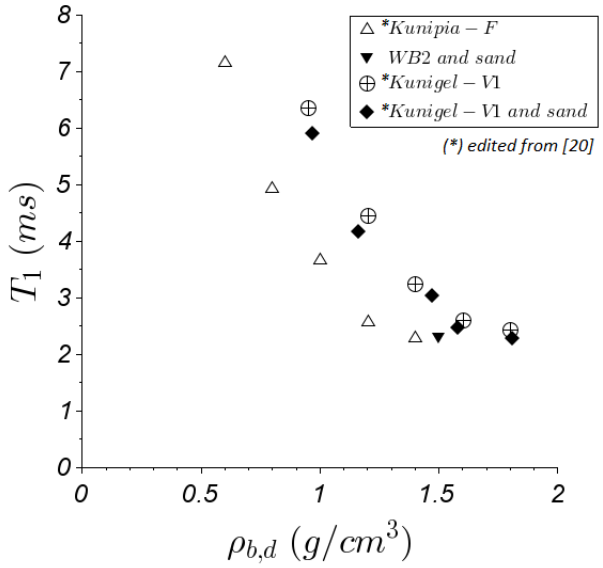

Fig. 4 Longitudinal relaxation time (T_1) as a function of the bentonite dry density ($\rho_{d,b}$) at 30 °C.

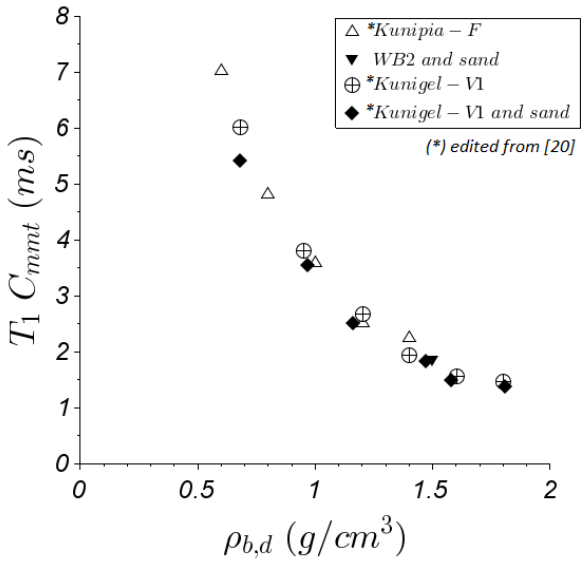

Fig. 5. Longitudinal relaxation time (T_1) relative to the montmorillonite content of the bentonite, as a function of the bentonite dry density ($\rho_{d,b}$) at 30 °C.

4 Conclusion

The proposed methodology set two main hypotheses which define the sand fraction influence on the water retention properties of a bentonite/sand mixture. They establish that sand does not contribute to water absorption capacity but only adds porosity to the mixture- gaps around sand grains-. As a result, bentonite occupy that porosity due to swelling.

From the hypotheses, two parameters are deduced: bentonite water content, w_b, and bentonite dry density, $\rho_{d,b}$. Their influence on water retention curves, studied for different mixtures -from pure bentonite to 20/80 bentonite/sand proportions-, is reported to be similar to the influence of usual water content and dry density parameters on pure bentonite. The similar values of w_b found at suctions bigger than 9 MPa, the dependence on $\rho_{d,b}$ to define the transition point of the WRC, and the correct estimation of w_b^{sat}, -dependent of $\rho_{d,b}$- imply that the hypotheses are validated.

Moreover, NMR relaxometry tests on bentonite/sand mixtures at saturation state show no differences to tests run on pure bentonite. This fact validates the hypotheses as well.

Therefore, it is concluded that sand, even at high concentrations (80% on dry mass), does not influence in the water retention properties. The mixture can be considered as an equivalent pure bentonite specimen whose dry density is equal to $\rho_{d,b}$, and whose WRC is defined by w_b. The use of these parameters has been proved to be useful and practical on water retention characterization. However, this simplification may not be applicable to other hydromechanical properties.

In order to compare NMR relaxometry results for different mixtures, an original methodology based on its dependency on $\rho_{d,b}$ and its montmorillonite content has been validated. It highlights the ability to predict longitudinal relaxation times (T_1) for bentonite/sand mixtures and even pure bentonite.

References

1. H. Komine, N. Ogata, Can. Geotech. J. **31 (4)**, 478-490 (1994)
2. D. Arnedo, E. E. Alonso, S. Olivella, E. Romero, Phys. Chem. Earth **33 (S1)**, S237-S247 (2008)
3. Q. Wang, A. M. Tang, Y. J. Cui, P. Delage, J. D. Barnichon, W. M. Ye, Soils Found. **53 (2)**, 232-245 (2013)
4. M.N. Gray, S. C. H. Cheung, D.A. Dixon, AECL 7825 (1984)
5. M. Fleury, R. Fabre, J. B. W. Webber, *Comparison of pore size distributions by NMR relaxation and NMR cryoporometry in shales*, in International Symposium of the Society of Core Analysts, ISSCA, 16-21 August 2015, St. John's Newfound and Labrador, Canada (2015)
6. A.M. Tang, Y. J. Cui, Can. Geotech. J. **42 (1)**, 287-296 (2005)
7. P. F. Faure, S. Rodts, Magn. Reson. Imaging **26 (8)**, 1183-1196 (2008)
8. S. W. Provencher, Comput. Phys. Commun. **27 (3)**, 213-227 (1982)
9. H. Penvern, M. Zhou, B. Maillet, D. Courtier-Murias, M. Scheel, J. Perrin, T. Weitkamp, S. Bardet, S. Caré, P. Coussot, Phys. Rev. Appl. **14**, 054051 (2020)
10. J. O. Lee, W. J. Cho, K. S. Chun, Nucl. Eng. Technol. **31 (2)**, 139-150 (199)
11. S. S. Agus, T. Schanz, D. G. Fredlund, Can. Geotech. J. **3(2)**, 125-137 (2008)
12. G. D. Morena, V. Navarro, L. Asensio, D. Gallipoli, Acta Geotech. **16**, 2775–2790 (2021)
13. D. Manca, *Hydro-chemo-mechanical characterization of sand/bentonite mixtures: with a focus on the water and gas transport properties,* EPFL (2015)
14. A. M. Tang, Y. J. Cui, JRMGE **2(1),** 91-96 (2010)
15. M. Fleury, E. Kohler, F. Norrant, S. Gautier, J. M'Hamdi, L. Barré, J. Phys. Chem. C **117 (9)**, 4551-4560 (2013)
16. T. R. Todoruk, C. K. Langford, A. Kantzas, Environ . Sci. Technol. **37**, 2707-2713 (2003)
17. H. Tian, C. Wei, R. Yan, Appl. Clay Sci. **170**, 106-113 (2019)
18. G. Xie, Y. Xiao, M. Deng, Q. Zhang, D. Huang, L. Jiang, Y. Yang, P. Luo, ENFUEM **33**, 9067-9073 (2019)
19. A. Seiphoori, A. Ferrari, L. Laloui, Geotechnique **64 (9)**, 721-734 (2014)
20. T. Okhubo, H. Kikuchi, M. Yamaguchi, Phys Chem Earth **33(1)**, S169-S176 (2008)
21. S. Rongwei, T. Tsukahara, ACS Earth Space Chem. **4**, 535-544 (2020)